Control of Wheeled Mobile Manipulators with Flexible Suspension Considering Wheels Slip Effects

Rambod Rastegari [a,*], Khalil Alipour [b]

[a] Department of Mechanical Engineering, Islamic Azad University, Parand Branch, Parand, Iran
[b] Department of Mechatronics Engineering, Faculty of New Sciences and Technologies, University of Tehran, Tehran, Iran

Received 11 January 2017; revised 20 March 2017; accepted 18 May 2017; available online 16 October 2017

Abstract

Wheeled mobile manipulators utilize both the locomotion capabilities of the wheeled platform and manipulation capacity of the arm. While the modelling and control of such systems have previously been studied, most of them have considered robots with rigid suspension and their wheels are subject to pure rolling conditions. To relax the aforementioned limiting assumptions, this research addresses modelling and control of a mobile manipulator with flexible suspension while considers the frictional effects. To this end, the Newton-Euler approach is employed and the modelling process is elaborated. To control the system, a two degree-of-freedom policy is suggested at two levels. In the first level, the Multiple Impedance Control (MIC) algorithm is modified and then is effectively utilized. Next, in the second level, the wheels actuating torques are adjusted such that the required forces/torques of the platform resulted from the first level be realized. The obtained simulation results support the proficiency of the suggested control scenario to control of wheeled mobile robots with flexible suspension and pneumatic tires.

Keywords: *Space Explorations, Mobile Robots, Wheeled Robots, Multiple Impedance Control.*

1. Introduction

In the future, the robotic systems will be utilized in various applications ranging from object manipulation and surgery to space exploration [1-3]. The use of robotic systems for deep space exploration and exact missions can dramatically reduce the cost, [3]. Today, there are various kinds of structures in the robotic systems. In terms of mobility of the base, the robot systems are divided into two categories, i.e. fixed-base and mobile robots. In contrast to the fixed-base robots, the mobile robots have an infinite workspace. Consequently, such kind of systems have absorbed much of interest. One of the main robot structures is Wheeled Mobile Robots (WMRs). The various advantages of WMRs have made them appropriate for a wide range of space and terrestrial applications. The mars rover is an instant which has presented successfully its benefits for exploration and performing experiments on mars, Figure 1.Due to features and vast applications of WMRs, many researches have been focused on them [4].

The kinematics, kinetics and control of car-like WMRs have been discussed in [5]. To validate the obtained dynamics, various matrices in the model have been obtained in two ways. Then the results of the aforementioned methods have been compared to verify the obtained model. Using the

* Corresponding author. Email: r_rastegari@piau.ac.ir

formulation of virtual work, the explicit dynamics of a car-like WMR subject to non-slip condition has been derived, [6]. The suggested approach is general and can be utilized for various types of nonholonomic WMRs.

In [7], dynamics of a robot with differentially driven wheels which is equipped with multiple arm has been derived. Besides, the system has been controlled using MIC algorithm. In some of references [8-9], the kinematics/kinetics and control of wheeled robots with single or multiple trailers were reported.

Despite of the aforementioned studies, in all of them it has been assumed that the robots wheels are subject to pure rolling. As a result, the friction force has not been appeared in the equations of motion. Hence, in some of the recent studies, a more realistic model which include the slip/skid are proposed [10-12]. However, these recent works do not consider a flexible suspension for the system.

In the context of wheeled mobile manipulators, few works [13-15] exist which consider the robot with flexible suspension. However, in [13] and [14], the robot is constrained with the pure rolling condition and in [15], the robot control has not been performed while considering the tire friction model.

In the current study, the dynamics of a wheeled robot during planar motions is studied. The robot has pneumatic tires and has flexible suspension. To model the tire friction forces, the Dugoff equations are employed. Also, considering the wheels actuation torques as control inputs, a new two-layer controller is suggested. In the first layer, the robot motion is adjusted using the modified MIC method and in the second layer, which will be called the local controller, the wheel actuation torques are obtained such that the required forces/toques of the first layer be realized.

After this introduction, in section 2, the robot model with flexible suspension is presented while the friction model of the tires and slip effects are addressed. In section 3, the control scenario is elaborated. Toward this goal, first in the first control level the MIC law is modified due to existence of passive joints. Furthermore, in the second control level, the main control inputs to achieve the first layer outputs are calculated. The obtained simulation results, in section 4, support the merits of the novel control architecture for wheeled robots in planar maneuvers.

2. Modeling the Robot Dynamics

2.1. Deriving the Equations of Motion in Planar Movement

In the present section, the aim is to derive the dynamics of a planar wheeled mobile manipulator. To this end, first, the explicit slippage effects between the tires and ground are neglected. After that, the aforementioned effects are considered in the model. Also, for determining some of the initial values of the system generalized coordinates, the system equilibrium equations are employed.

Fig. 1. NASA wheeled robot for space exploration

2.2. Determining the Generalized Coordinates in Static Equilibrium

Consider a wheeled mobile manipulator as illustrated in Figure 2. The considered robot includes a chassis which is mounted on wheels and can move on level and uneven ground along x and y directions and rotate about the vertical line normal to the plane of motion. Additionally, a robot with revolute joint is connected to the platform. Figure 2 shows the system in static equilibrium. Assume that the chassis after loading, the chassis center of mass has moved Y_0 downward. Also, the chassis is rotated θ_0 counterclockwise. In Figure 2, the variable H represents the chassis center of mass height relative to the wheel center when the suspension springs are with the natural length. In addition, L denotes the robot arm length and the other robot parameters are demonstrated in Figures 2 and 3. Besides, L_0 indicate the wheel base. Initial angle of the arm relative to robot chassis is considered as $\psi_0 = 45^{\circ}$. The free lengths of suspension springs are considered to be equal. The variables in dynamic status are measured with respect to their values in static condition. It is worth to mention that the variable Y is measured with respect to the static equilibrium and its sign is considered positive in upward direction. Notice that the variable $\theta_0 + \theta$ represents the instantaneous chassis posture relative to the horizontal direction during motion.

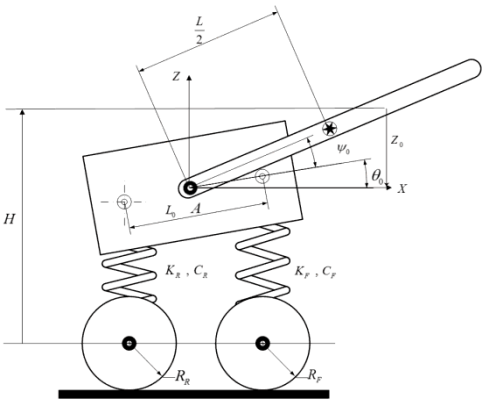

Fig. 2. Wheeled planar robot in static equilibrium situation

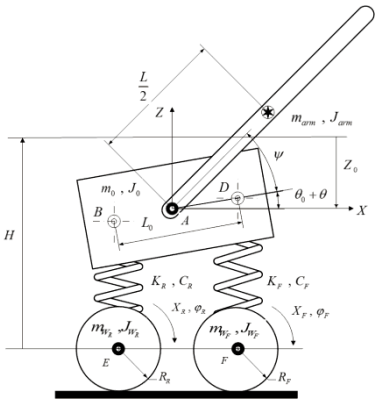

Fig. 3. Wheeled planar robot in general situation

The equilibrium equations in static case, to determine some variables, can be written as

$$\sum F = 0 \quad \Rightarrow F_{SR} + F_{SF} - (m_0 + m_{arm})g = 0 \tag{1}$$

$$\sum M_A = 0 \quad \Rightarrow -F_{SR} \times \frac{L_0}{2}\cos\theta_0 + F_{SF} \times \frac{L_0}{2}\cos\theta_0 - m_{arm} g \frac{L}{2}\cos(\theta_0 + \psi_0) = 0 \tag{2}$$

Where,F_{SF} and F_{SR} indicate the forces applied to the chassis at front and rear, respectively. In Eq. (2), the effect of traction force is neglected. The exerted forces at the front and rear of chassis due to suspension can be written as

$$F_{SF} = K_F\left(Z_0 - \frac{L_0}{2}\sin\theta_0\right) \tag{3}$$

$$F_{SR} = K_R\left(Z_0 + \frac{L_0}{2}\sin\theta_0\right) \tag{4}$$

By substitution of Eqs. (3) and (4) into (1) and (2), the values of Z_0 and θ_0 can be obtained.

2.3. Deriving the Dynamic Equation without Considering the Friction Model

In Figure 3, the robot during travel is shown. The suspension forces at the rear and front of the vehicle can be written as

$$F_{SF} = K_F\left(Z_0 - Z - \frac{L_0}{2}\sin(\theta_0 + \theta)\right) \tag{5}$$

$$F_{SR} = K_R\left(Z_0 - Z + \frac{L_0}{2}\sin(\theta_0 + \theta)\right) \tag{6}$$

Also, the position vector of the arm can be calculated as

$$x_{arm} = X_p + \frac{L}{2}\cos(\psi + \theta + \theta_0) \tag{7}$$

$$z_{arm} = Z_p + \frac{L}{2}\sin(\psi + \theta + \theta_0) \tag{8}$$

To examine the robot in dynamic condition, it is necessary to obtain the Jacobian between task and joint spaces. In this regard, the task space variables can be considered as

$$\mathbf{X} = \begin{Bmatrix} X_p \\ \theta \\ z_{arm} \end{Bmatrix} \tag{9}$$

Moreover, the joint space variables are as

$$\mathbf{q} = \begin{Bmatrix} X_p \\ Z_p \\ \theta \\ \psi \end{Bmatrix} \tag{10}$$

By differentiating of Eqs. (8) and (9) and considering the joint and task spaces as Eqs. (9) and (10), the robot Jacobian is calculated as

$$J = \begin{bmatrix} 1 & 0 & 0 & 0 \\ 0 & 0 & 1 & 0 \\ 0 & 1 & \frac{L}{2}\cos(\theta + \theta_0 + \psi) & \frac{L}{2}\cos(\theta + \theta_0 + \psi) \end{bmatrix} \tag{11}$$

Additionally, by twice differentiating from Eqs. (7) and (8), the arm center of mass acceleration is obtained as

$$\ddot{x}_{arm} = \ddot{X}_p - \frac{L}{2}(\ddot{\psi} + \ddot{\theta})\sin(\psi + \theta + \theta_0)\frac{L}{2}(\dot{\psi} + \dot{\theta})^2\cos \times (\psi + \theta + \theta_0) \tag{12}$$

$$\ddot{z}_{arm} = \ddot{Z}_p + \frac{L}{2}(\ddot{\psi} + \ddot{\theta})\cos(\psi + \theta + \theta_0)\frac{L}{2}(\dot{\psi} + \dot{\theta})^2\sin \times (\psi + \theta + \theta_0) \tag{13}$$

Considering D'Alembert principle, the system dynamic equations along x and z is written in the following form.

$$\sum F_x = 0 \quad \Rightarrow \quad F_T - m_0\ddot{X}_p - m_{arm}\ddot{x}_{arm} = 0 \tag{14}$$

$$\sum F_z = 0 \quad \Rightarrow \quad -m_0\ddot{Z}_p - m_{arm}\ddot{z}_{arm} + F_{SF} + F_{SR} - (\mathrm{m}_0 + \mathrm{m}_{arm})\mathrm{g} = 0 \tag{15}$$

In the above relations, F_T is traction force which is generated due to the friction between tire and ground? The third equation is obtained for the robot arm by writing the moment about the point 'A' which is written as

$$\begin{aligned}&\sum M_A = 0 \quad \Rightarrow \quad \tau_{arm} - m_{arm}g\frac{L}{2}\cos(\theta_0 + \theta + \psi)\\ &+m_{arm}\ddot{x}_{arm}\frac{L}{2}\sin(\theta_0 + \theta + \psi)\\ &\times m_{arm}\ddot{z}_{arm}\frac{L}{2}\cos(\theta_0 + \theta + \psi)\\ &\times \ddot{z}_{arm} \ -J_{arm}(\ddot{\theta} + \ddot{\psi}) = 0\end{aligned} \tag{16}$$

The fourth equation is obtained by writing the moment about the chassis center of mass which can be written as

$$\begin{aligned}&\sum M_A = 0 \quad \Rightarrow \quad -\tau_{arm} + F_{Sus_F}\frac{L_0}{2}\cos(\theta_0 + \theta)\\ &-F_{Sus_R}\frac{L_0}{2}\cos(\theta_0 + \theta) - J_0\ddot{\theta} + M_T = 0\end{aligned} \tag{17}$$

Where, M_T denotes the moments due to friction force and its computation will be elaborated later. By substituting Eqs. (12) and (13) into Eqs. (14)- (17) and substituting τ from Eq. (16) into (17), the robot equations of motion without considering the explicit modeling of wheels are obtained as

$$\boldsymbol{M}\ddot{\boldsymbol{q}} + \boldsymbol{C} + \boldsymbol{G} = \boldsymbol{\Gamma}^T\boldsymbol{Q}_m = \begin{Bmatrix} F_T \\ 0 \\ \tau \\ M_T \end{Bmatrix} \tag{18}$$

Where,

$$\boldsymbol{\Gamma} = \begin{bmatrix} 1 & 0 & 0 & 0 \\ 0 & 0 & 1 & 0 \\ 0 & 0 & 0 & 1 \end{bmatrix} \tag{19}$$

And

$$\boldsymbol{Q}_m = \begin{Bmatrix} F_T \\ \tau \\ M_T \end{Bmatrix} \tag{20}$$

In Eq. (20), the components of F_T and M_T can be obtained based on the friction forces produced at the wheels/ground contact areas. In the subsequent material, for completion of robot equations of motion, the dynamics of front and rear wheels and the mutual interaction moment between the suspension and wheels along with frictional force effects are considered.

2.4. Augmenting the Wheels Dynamics to the Robot Equations

In Eqs. (18), it is required that the forces and moment generated due to frictional forces be considered. Toward this goal, considering Figure 3, the relevant forces and moment due to the friction can be obtained as

$$F_T = F_{R_X} + F_{F_X} \tag{21}$$

The position vector of rear and front axle forces can be written as

$$\vec{r}_R = -\left(\frac{L_0}{2}\cos(\theta + \theta_0)\right)\hat{\imath} - \left(H_1 - Z_0 + Z - \frac{L_0}{2}\sin(\theta_0 + \theta)\right)\hat{\jmath} \tag{22}$$

$$\vec{r}_F = \left(\frac{L_0}{2}\cos(\theta + \theta_0)\right)\hat{\imath} - \left(H_1 - Z_0 + Z + \frac{L_0}{2}\sin(\theta_0 + \theta)\right)\hat{\jmath} \tag{23}$$

Exploiting the free-body diagram of Figure 4, the moment effect of applied forces at axles about chassis center of mas can be calculated as

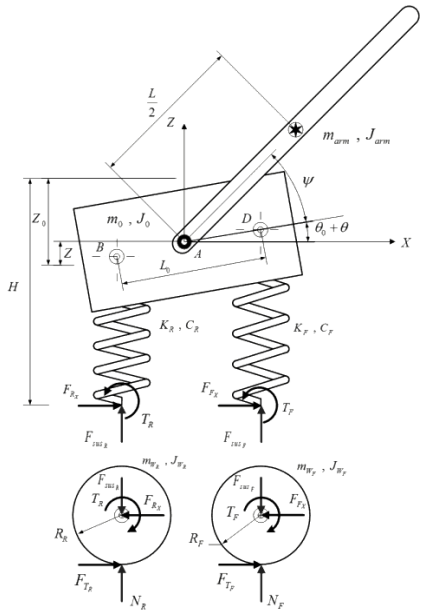

Fig. 4. Free body diagram of wheeled planar robot with considering the effects of wheels and friction forces

$$\begin{aligned}&M_T = \vec{r}_R \times \vec{F}_{R_X} + \vec{r}_F \times \vec{F}_{F_X} =\\ &-F_{R_X}\left(H_1 - Z_0 + Z - \frac{L_0}{2}\sin(\theta + \theta_0)\right)\\ &-F_{F_X}\left(H_1 - Z_0 + Z + \frac{L_0}{2}\sin(\theta + \theta_0)\right)\end{aligned} \tag{24}$$

Eqs. (21) and (24) can be written in matrix format as

$$\begin{bmatrix} 1 & 1 \\ \alpha_1 & \alpha_2 \end{bmatrix}\begin{Bmatrix} F_{R_X} \\ F_{F_X} \end{Bmatrix} = \begin{Bmatrix} F_T \\ M_T \end{Bmatrix} \tag{25}$$

Where,

$$\alpha_1 = -\left(H - Z_0 + Z - \frac{L_0}{2}\sin(\theta + \theta_0)\right)$$
$$\alpha_2 = -\left(H - Z_0 + Z + \frac{L_0}{2}\sin(\theta + \theta_0)\right) \quad (26)$$

As a result, to determine the value of F_T and M_T, it is sufficient that the values of$F_{R_X}$and F_{F_X}be specified. To this end, the equations of front and rear wheels in Figure 4 can be written as

$$\begin{cases} -F_{R_X} + F_{T_R} - m_{W_R}\ddot{X}_R = 0 \\ N_R - F_{R_Y} = 0 \\ T_R - F_{T_R}R_R - J_{W_R}\ddot{\phi}_R = 0 \end{cases} \quad (27)$$

$$\begin{cases} -F_{F_X} + F_{T_F} - m_{W_F}\ddot{X}_F = 0 \\ N_R - F_{R_Y} = 0 \\ T_F - F_{T_F}R_R - J_{W_F}\ddot{\phi}_F = 0 \end{cases} \quad (28)$$

In Eqs. (27) and (28), it is needed that the acceleration of front and rear wheels center of mass be written in terms of the robot generalized coordinates. To this end, first the positions of wheels center of mass along horizontal axis are written as

$$X_F = X_p + \frac{L_0}{2}\cos(\theta_0 + \theta)$$
$$X_R = X_p - \frac{L_0}{2}\cos(\theta_0 + \theta) \quad (29)$$

By twice differentiation, we have

$$\ddot{X}_F = \ddot{X}_p - \frac{L_0}{2}\dot{\theta}^2\cos(\theta_0 + \theta) - \frac{L_0}{2}\ddot{\theta}\sin(\theta_0 + \theta)$$
$$\ddot{X}_R = \ddot{X}_p + \frac{L_0}{2}\dot{\theta}^2\cos(\theta_0 + \theta) + \frac{L_0}{2}\ddot{\theta}\sin(\theta_0 + \theta) \quad (30)$$

By substituting of Eqs. (30) into (27) and (28), the values of the required forces in Eqs. (25) are obtained as

$$F_{F_X} = F_{T_F} - m_{W_F}\left(\ddot{X}_p - \frac{L_0}{2}\dot{\theta}^2\cos(\theta_0 + \theta) - \frac{L_0}{2}\ddot{\theta}\sin(\theta_0 + \theta)\right)$$
$$F_{R_X} = F_{T_R} - m_{W_R}\left(\ddot{X}_p + \frac{L_0}{2}\dot{\theta}^2\cos(\theta_0 + \theta) + \frac{L_0}{2}\ddot{\theta}\sin(\theta_0 + \theta)\right) \quad (31)$$

Consequently, if frictional forces at the front and rear wheels are known, then the values of F_T and $M_T$can be obtained. Moreover, based on the third relation of Eqs. (27) and (28), the rotational dynamics of wheels is written as

$$T_R = F_{T_R}R_R + J_{W_R}\ddot{\phi}_R \quad (32)$$

$$T_F = F_{T_F}R_R + J_{W_F}\ddot{\phi}_F \quad (33)$$

To compute $F_{T_R}$and F_{T_F} Dugoff equations are utilized as it will be described in detail in the subsequent section.

2.5. Calculation of Friction Forces based on Dugoff Model

In the dynamic model obtained in the former subsection, it is inevitable to compute the friction forces generated at the ground/wheels contact patches. Herein, considering pneumatic tires, the Dugoff model is utilized to calculate the frictional forces. It is stressed that the assumption of wheel pure rolling is just valid once the system weight is low and the robot velocity and acceleration are not significant [21]. Consequently, modeling of the mobile robotic system while considering the tire slippage is completely justified. In Figure 5, the top view of the platform in a general case is depicted.

The side slip angle is defined as the angle between the wheel center velocity vector and the wheel plane. Consequently knowing the lateral component of the i-th wheel center velocity v_{iy} and the longitudinal component of the aforementioned velocityv_{ix}, the side slip angle is written as

$$\beta_i = \tan^{-1}\left(\frac{v_{iy}}{v_{ix}}\right) - \delta_i \quad ; i = 1, \dots, 4 \quad (34)$$

Where, δ_i indicate the wheel steering angle. If the longitudinal and lateral components of tire center velocity are substituted in terms of velocity components of reference point C_0, then the side slip angle for various tires are attained as

$$\beta_1 = \tan^{-1}\left(\frac{-\dot{X}_p s\varphi + \dot{Y}_p c\varphi + L_F\dot{\varphi}}{\dot{X}_p c\varphi + \dot{Y}_p s\varphi + W_R\dot{\varphi}}\right) - \delta_1$$
$$\beta_2 = \tan^{-1}\left(\frac{-\dot{X}_p s\varphi + \dot{Y}_p c\varphi + L_F\dot{\varphi}}{\dot{X}_p c\varphi + \dot{Y}_p s\varphi - W_L\dot{\varphi}}\right) - \delta_2$$
$$\beta_3 = \tan^{-1}\left(\frac{-\dot{X}_p s\varphi + \dot{Y}_p c\varphi - L_B\dot{\varphi}}{\dot{X}_p c\varphi + \dot{Y}_p s\varphi + W_R\dot{\varphi}}\right) - \delta_3$$
$$\beta_4 = \tan^{-1}\left(\frac{-\dot{X}_p s\varphi + \dot{Y}_p c\varphi - L_B\dot{\varphi}}{\dot{X}_p c\varphi + \dot{Y}_p s\varphi - W_L\dot{\varphi}}\right) - \delta_4 \quad (35)$$

Where in the above relations, φ represents the robot heading angle which is set zero for longitudinal maneuvers. Tire slip ratio is also defined as

$$s_i = \frac{V_i - R_e\omega_i}{V_i} \quad ; R_e\omega_i < V_i$$
$$s_i = \frac{V_i - R_e\omega_i}{R_e\omega_i} \quad ; R_e\omega_i \geq V_i \quad (36)$$

where, R_e indicates the tire effective radius [22], ω_i denotes the angular velocity of the i-th wheel and V_i is the component of the linear velocity of the wheel center in the wheel plane. Tire forces can be obtained using the following simplified model [22].

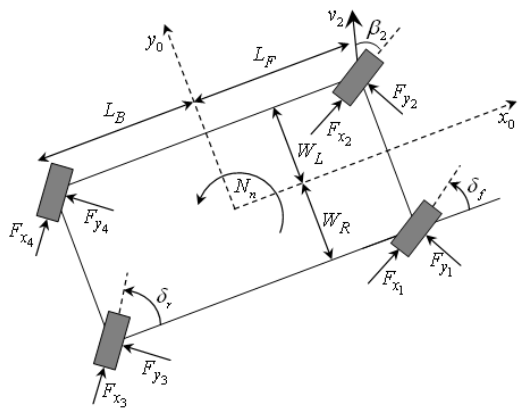

Fig. 5. Platform top view by considering the applied forces on tires

$$F_{x_i} = -f_i C_{x_i} s_i$$
$$F_{y_i} = -f_i C_{y_i} \beta_i \quad (37)$$

Where,

$$f_i = \begin{cases} 1 & ; F_{R_i} \le \frac{\mu_i F_{z_i}}{2} \\ \left(2 - \frac{\mu_i F_{z_i}}{2F_{R_i}}\right)\frac{\mu_i F_{z_i}}{2F_{R_i}} & ; F_{R_i} > \frac{\mu_i F_{z_i}}{2} \end{cases} \quad (38)$$

$$F_{R_i} = \sqrt{\left(C_{x_i} s_i\right)^2 + \left(C_{y_i}\beta_i\right)^2} (i = 1, \dots, 4) \quad (39)$$

In the above equations, F_{z_i} denotes the tire normal forces and depends on robot weight, the forces/torques exerted to the chassis by the arm and the longitudinal/lateral acceleration of the robot chassis. μ_i is the slip coefficient. Also, C_{x_i} and C_{y_i} denote the tire stiffness along longitudinal and lateral directions, respectively.

The above equations are exploited for the planar motion case study in which the steering angles are considered to be fixed and the side slip angels are neglected.

3. Control of Wheeled Mobile Manipulator in Planar Movement

The initial controller which was chosen to robot control is MIC algorithm [23]. The reason of this selection is the flexibility of this control method to control fixed-base and mobile robots and even good performance during object manipulation even in the presence of flexibility inherent in the system. As we know the platform control inputs are wheel actuating torques. Also, the number of the degrees of the platform is less than its actuators. In this study, position control of chassis along horizontal axis, of its pitch angle and control of the arm center of mass height via three control inputs, two wheels actuating torques and arm joint torque, are desired. To this end, due to passivity of chassis motion along vertical axis, first the MIC control law is modified.

3.1. Modification of MIC in the Case of Passive Joints

As mentioned in [23], the MIC law should be applied to all the robot joints. In case of existence of passive joints, it is not possible to provide the force/torque commanded by MIC law. Consequently, the modification of MIC law in the current situation is required. To this end, it is needed that the active and passive degrees of freedom of robot be specified. In this regards, the matrix $\boldsymbol{\Gamma}$ is considered which defines between joint space variables vector and actuator space as follows.

$$\dot{\boldsymbol{q}}_{act} = \boldsymbol{\Gamma}\ \dot{\boldsymbol{q}} \quad (40)$$

In the above relation, $\dot{\boldsymbol{q}}$ is the joint space variables vector with the dimension $n \times 1$ and $\dot{\boldsymbol{q}}_{act}$ denotes the active joints vector of dimension $m \times 1$ where $m < n$. In this matrix, the column associated with the passive joints are completely zero. It is worth mentioning that the number of operational space coordinates is considered to be equal with the number of active joint variables. Therefore, the Jacobian between the joint space coordinates and task space coordinates is a non-square matrix of dimension $m \times n$ and

$$\dot{\tilde{\boldsymbol{X}}} = \boldsymbol{J}\dot{\boldsymbol{q}} \quad (41)$$

Based on the virtual work principle, it is possible to write the following force/torque relation between the joint and task spaces

$$\boldsymbol{Q}^T_{m\,act}\dot{\boldsymbol{q}}_{act} = \tilde{\boldsymbol{Q}}^T_m \dot{\tilde{\boldsymbol{X}}} \quad (42)$$

Note that in case of existence of flexible members in the system, the above relation is correct provided that the displacement of the two ends of such members can be neglected. By substituting of Eqs. (40) and (41) into Eq. (42), we have

$$\boldsymbol{Q}^T_{m\,act}\boldsymbol{\Gamma} = \tilde{\boldsymbol{Q}}^T_m \boldsymbol{J} \quad (43)$$

If the transposed of the above relation is written, then by premultiplication of it by $\boldsymbol{\Gamma}^T$, the following result is obtained.

$$\boldsymbol{Q}_{m_{act}} = \boldsymbol{\Gamma J}^T \widetilde{\boldsymbol{Q}}_m \tag{44}$$

It is pointed out that

$$\boldsymbol{\Gamma \Gamma}^T = \boldsymbol{I}_{m \times m} \tag{45}$$

The equations of motion of a mobile robot in the case that it does not have any interaction with the environment can be written as

$$\boldsymbol{H\ddot{q}} + \boldsymbol{C} + \boldsymbol{G} = \boldsymbol{J}^T \widetilde{\boldsymbol{Q}}_m \tag{46}$$

By differentiation of Eq. (41), the following relation can be obtained.

$$\ddot{\boldsymbol{q}} = \boldsymbol{J}^{\#}\left(\ddot{\tilde{\boldsymbol{X}}} - \dot{\boldsymbol{J}}\dot{\boldsymbol{q}}\right) \tag{47}$$

By substituting of Eq. (46) into (51) and premultiplication of both sides of the resulted equation by $\boldsymbol{\Gamma}$, the following result is obtained.

$$\boldsymbol{\Gamma}\left[\boldsymbol{HJ}^{\#}\left(\ddot{\tilde{\boldsymbol{X}}} - \dot{\boldsymbol{J}}\dot{\boldsymbol{q}}\right) + \boldsymbol{C} + \boldsymbol{G}\right] = \boldsymbol{\Gamma J}^T \widetilde{\boldsymbol{Q}}_m \tag{48}$$

premultiplying of Eq. (48) By term $(\boldsymbol{\Gamma J}^T)^{-1}$ leads to the following equation.

$$\widetilde{\boldsymbol{H}}_{final}\ddot{\tilde{\boldsymbol{X}}} + \widetilde{\boldsymbol{C}}_{final} + \widetilde{\boldsymbol{G}}_{final} = \widetilde{\boldsymbol{Q}}_m \tag{49}$$

Where,

$$\widetilde{\boldsymbol{H}}_{final} = (\boldsymbol{\Gamma J}^T)^{-1}(\boldsymbol{\Gamma H})\boldsymbol{J}^{\#} \tag{50}$$

$$\begin{aligned}\widetilde{\boldsymbol{C}}_{final} &= (\boldsymbol{\Gamma J}^T)^{-1}\boldsymbol{\Gamma C} - (\boldsymbol{\Gamma J}^T)^{-1}(\boldsymbol{\Gamma H})\boldsymbol{J}^{\#}\dot{\boldsymbol{J}}\dot{\boldsymbol{q}} \\ &= (\boldsymbol{\Gamma J}^T)^{-1}\boldsymbol{\Gamma C} - \widetilde{\boldsymbol{H}}_{final}\dot{\boldsymbol{J}}\dot{\boldsymbol{q}}\end{aligned} \tag{51}$$

$$\widetilde{\boldsymbol{G}}_{final} = (\boldsymbol{\Gamma J}^T)^{-1}\boldsymbol{\Gamma G} \tag{52}$$

Note that, Eq. (49) denotes the robot equation in the task space level. Considering the output error as$\tilde{\boldsymbol{e}} = \tilde{\boldsymbol{X}}_d - \tilde{\boldsymbol{X}}$, the following control law is obtained in the task level

$$\widetilde{\boldsymbol{Q}}_m = \widetilde{\boldsymbol{H}}_{final}\boldsymbol{M}_{des}^{-1}\left(\boldsymbol{M}_{des}\ddot{\tilde{\boldsymbol{X}}}_d + \boldsymbol{K}_d\dot{\tilde{\boldsymbol{e}}} + \boldsymbol{K}_p\tilde{\boldsymbol{e}}\right) + \widetilde{\boldsymbol{C}}_{final} + \widetilde{\boldsymbol{G}}_{final} \tag{53}$$

Note that in Eq. (53), $\ddot{\tilde{\boldsymbol{X}}}_d$represents the desired acceleration in the task space. Also, $\boldsymbol{K}_d$ and $\boldsymbol{K}_p$are gain matrices which are associated with the velocity and position error at the task space level, respectively.

3.2. Two Degree-of-Freedom Control Law for Planar WMR

As shown in Figure 6, the robot control strategy is a 2 degree-of-freedom scenario. In the first level, using the modified MIC law algorithm developed in the previous section, the desired required force along X axis, F_X, pitch angle torque, τ_θ, and required torque at the arm joint, τ_{arm}, are calculated. After that F_X and τ_θ are considered as set-point for the second control level, which is called local controller, by which the wheels actuating torques are adjusted.

The structure of local control is formed based on Eq. (25). Based on this relation, the desired traction forces which should be generated at the contact of wheels/ground are first produced as

$$\begin{bmatrix}F_f^{des} \\ F_r^{des}\end{bmatrix} = B^{-1}\begin{bmatrix}F_X \\ \tau_\theta\end{bmatrix} \tag{54}$$

$$B = \begin{bmatrix}1 & 1 \\ \alpha_1 & \alpha_2\end{bmatrix}$$

The goal is that the actuating torques of wheels, i.e. T_r and T_f, should be provided such that the traction forces, i.e. $F_{R_X}$and F_{F_X}, be equal to their desired values as much as possible. Consequently, it can be claim that the local controller is in fact an explicit force control strategy. Figure 6 illustrates the explicit force control of rear and front wheels. To regulate the wheel traction forces, a proportional controller is exploited as demonstrated in Figure 7. The local controller adjusts the actuating torques of wheels such that the longitudinal force and pitch angle torque required as set-points of MIC can be obtained. One of the interesting features of this proposed controller is that it does not require the complex model which in turn improves the local controller robustness against parametric and unstructured uncertainties of the robot model. It is worth mentioning that to implement the structure of the proposed 2 degree-of-freedom controller, a sensor or estimator of traction forces of wheels is essential. Notice that to estimate the traction forces, various studies exist, see for instance [19] and reference therein.

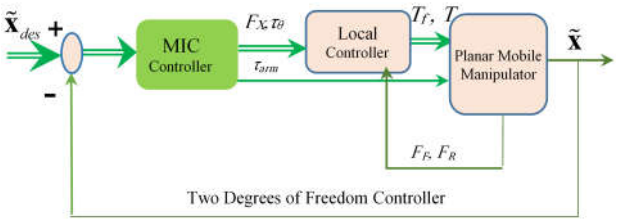

Fig. 6. The general architecture of the proposed controller

It should also be pointed out that in the joint space the robot has four independent degrees of freedom among which the motion of the robot along Y axis is passive. Consequently to control the robot motion, the modified MIC

method elaborated in subsection 3-1 will be utilized. Also, using the technique described in subsection 3-2, the task space variables are completely controlled.

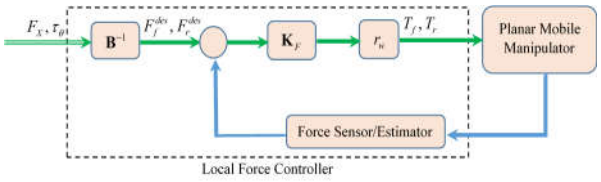

Fig. 7. Explicit force control for tuning of the torques applied on the wheels

Note that the stability of MIC has been proven in [20] using direct method of Lyapunov. Using some modifications, this proof can be extended to the proposed modified MIC. Also, by some analysis, it can easily be found that

$$F_{T_R} = \frac{K_F}{K_F + 1} F_r^{des} \tag{55}$$

By considering high values for gain K_F, it can be concluded that $F_{T_R} \cong F_r^{des}$. Consequently, the stability of the system can be guaranteed.

4. Simulation Results

In this section, the simulation results of control of a wheeled robot equipped with a single 1R-arm manipulator are discussed while it is moving on the Mars surface. Toward this goal, a system similar to Figure 3 is taken into account whose geometrical/mass specifications are as mentioned in Table 1. It should be emphasized that considering such parameters for the system leads to a 4 cm deflection of the suspension. In addition, they causes an under-damped response of the main platform.

Table. 1. The system and simulation specifications

Parameters	Unit	Value
m_0	kg	600
L_0	m	2
H_1	m	0.6
m_{arm}	kg	20
L	m	1
$K_f = K_r$	N/m	28700
$C_f = C_r$	Ns/m	2870
R_R	m	0.3
R_F	m	0.1
J_0	kgm^2	20
m_w	kg	10
μ_k	–	0.9

In Figures 8, 9 and 10 the actual and desired trajectories of the robot are illustrated. In these simulations, the output variables have been considered as $\tilde{\mathbf{X}} = [X \quad \theta \quad Z_{arm}]^T$. The gain matrices of the modified MIC are set as $\mathbf{M}_{des} = diag(1,1,1)$,$\mathbf{K}_d = diag(20,20,20)$,$\mathbf{K}_p = diag(200,200,200)$. Additional the control gains in the local control layer are chosen as $\boldsymbol{K}_F = diag(200,200)$.

In Figure 8, the motion of platform along x axis versus time is depicted. As seen the robot can track the desired trajectory.

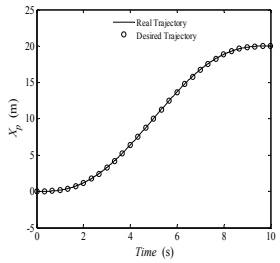

Fig. 8. The trajectory of the platform center of mass along x direction

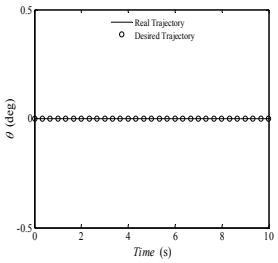

Fig. 9. The trajectory of platform pitch angle

In Figure 9, the actual and desired pitch angle of the mobile platform are shown. As it can be observed, after a short time, the robot can attain the desired pitch angle. It should be emphasized that this variable is passive and herein is controlled using the frictional forces of the wheels.

Figure 10 presents the variation of coordinate of manipulator arm in the vertical axis. As seen after 1 second from the initial of motion the error becomes zero and the desired trajectory is appropriately traced. In Figures 11 and 12, the wheels actuating torques are depicted.

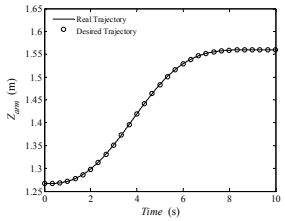

Fig. 10. The trajectory of the endeffector along vertical direction

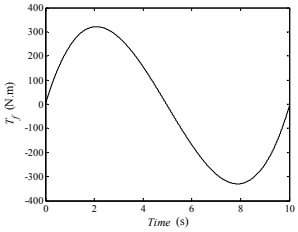

Fig. 11. The torque applied on the front wheel

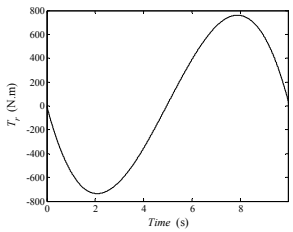

Fig. 12. The torque applied on the rear wheel

5. Conclusion

In the present paper, a robot with wheeled locomotion was taken into account. The robot has flexible suspension and equipped with pneumatic tires. Using Dugoff friction model, the whole system was modelled. Using a proposed two-layer control method, the adjusting the pitch angle of the platform was provided. In the first level of the controller, the motion of the robot using a modified MIC was regulated while in the second level the wheels actuating torques was provided such that the required forces/torques of the first level be realized. The obtained simulation results reveal the capabilities of the suggested controller for motion control of wheeled mobile manipulators with flexible suspension.

Acknowledgment

The authors would like to thank the financial support provided by Islamic Azad University, Parand branch for accomplishing this research.

References

[18] Tarvirdizadeh, B.; Yousefi-Koma, A., "Dynamic object manipulation by a flexible robotic arm: theory and experiment", Int. Journal of Robotics and Automation, Vol. 27, No. 3, pp. 263- 275 (2012).

[19] Hadi, A.; Akbari, H.; Tarvirdizadeh, B.; Alipour, K., "Developing a novel continuum module actuated by shape memory alloys" Sensors and Actuators A: Physical, Vol. 243, No. 1, pp.90-102 (2016).

[20] Moosavian, S. A. A.; Papadopoulos, E., "Free-flying robots in space: an overview of dynamics modelling, planning and control", Robotica, Vol. 25, No. 5, pp. 537–547 (2007).

[21] Salerno,A.; Angeles, J., "A new family of two-wheeled mobile robots: Modeling and controllability", IEEE Transactions on Robotics, vol. 23, pp. 169-173(2007).

[22] Moosavian, S.; Mirani, A., "Dynamics and Motion Control of Wheeled Robotic Systems", Esteghlal Journal of Engineering, Isfahan University of Technology, vol. 24, pp. 193-214 (2006). (In Persian)

[23] Yu, Q.; Chen, I.-M., "A general approach to the dynamics of nonholonomic mobile manipulator systems", Journal of dynamic systems, measurement, and control, vol. 124, pp. 512-521 (2002).

[24] Eslamy, M.; Moosavian, S. A. A., "Control of Suspended Wheeled Mobile Robots with Multiple Arms during Object Manipulation Tasks", IEEE Conference on Robotics and Automation, pp. 3730-3735 (2009).

[25] Khalaji, A. K.; Moosavian, S. A. A., "Dynamic modeling and tracking control of a car with n trailers", Multibody System Dynamics, Vol. 37, No. 2, pp. 211–225 (2016).

[26] Khanpoor, A.; Khalaji, A. K.; Moosavian, S. A. A., "Dynamics and Control of Wheeled Mobile Robot Attached by Trailer with Passive Spherical Wheels", Modares Mechanical Engineering, Vol. 15, No. 8, pp. 216-226 (2015). (In Persian).

[27] Low, C. B.; Wang, D., "Manoeuvrability and path following control of wheeled mobile robot in the presence of wheel skidding and slipping", Journal of Field Robotics, Vol. 27, No. 2, pp.127-144 (2010).

[28] Tian, Y.; Sarkar, N., "Control of a mobile robot subject to wheel slip", Journal of Intelligent and Robotic Systems, Vol. 74, No. 3-4, pp.915-929 (2014).

[29] Sidek, N.; Sarkar, N., "Exploiting wheel slips of mobile robots to improve navigation performance", Advanced Robotics, Vol. 27, No. 8, pp. 627–639 (2013).

[30] Eslamy, M.; Moosavian, S. A. A., "Dynamics Modelling of Suspended Mobile Manipulators: An Explicit Approach with Verification", International Journal of Modelling and Simulation, vol. 31,No. 2, pp. 112-119(2011).

[31] Eslamy, M.; Moosavian, S. A. A.,"Dynamics and cooperative object manipulation control of suspended mobile manipulators," Journal of Intelligent and Robotic Systems, vol. 60, pp. 181-199 (2010).

[32] Alipour, K.; Moosavian, S. A. A., "Effect of Terrain Traction, Suspension Stiffness and Grasp Posture on the Tip-over Stability of Wheeled Robots with Multiple Arms", Advanced Robotics, Vol. 26, pp. 817-842 (2012).

[33] Horiuchi, S.; Okada, K.; Nohtomi, S., "Effects of Integrated Control of Active Four Wheel Steering and Individual Wheel Torque on Vehicle Handling and Stability: A Comparison of Alternative Control Strategies", Vehicle System Dynamics Supplement, Vol. 33, pp. 680-691 (1999).

[34] Moosavian, S. A. A.; Papadopoulos, E., "Cooperative Object Manipulation with Contact Impact Using Multiple Impedance Control", International Journal of Control, Automation, and Systems, Vol. 8, No. 2, pp. 314-327 (2010).

[35] Albinsson, A.; Bruzelius, F.; Jacobson, B.; Fredriksson, J., "Design of tyre force excitation for tyre–road friction estimation", Vehicle System Dynamics, Vol. 55, No. 2, pp. 208-230 (2017).

[36] Moosavian, S. A. A.; Rastegari, R., "Multiple-Arm Space Free-Flying Robots for Manipulating Objects with Force Tracking Restrictions", Journal of Robotics and Autonomous Systems, Vol. 54, No. 10, pp. 779-788 (2006).